PNM Lab report

Giuseppe Filitto[1]

Abstract
This report is aimed to become familiarized with the NMR concepts learnt during the course and the lab experiences in which NMR apparata, signals with various sequences and real experimental data have been exploited. The first part of this report concerns theory main concepts about NMR, such as relaxometry and diffusion. Then in the Materials and Methods Section the main apparata will be analyzed, focusing on the portable NMR MOUSE. The last but not least part, Results and Discussion, is aimed to shown and to analyze the performed acquisitions and real experimental data, using the theory presented in the first section.

[1] *DIFA Department, Alma Mater Studiorum, Bologna, Italy*
*__Corresponding author__: giuseppe.filitto@studio.unibo.it

Contents

1. Introduction

Nuclear Magnetic Resonance (NMR) is a physical phenomenon which occurs when nuclei are immersed in a static magnetic field and subjected to a second oscillating magnetic field.
It was first described by Isidor Rabi who won the Nobel Price in Physics in 1944, using a molecular beam in a vacuum where where individual nuclei were isolated from each another and their environment, but it would not be until late 1945 that independent teams led by Felix Bloch at Stanford and Edward Mills Purcell at the MIT, would demonstrate NMR in water and paraffin.
The advantage of this technique lies in its wide range of applications, from chemistry to medicine, from industry to Cultural Heritage. As a matter of fact, there are many different techniques and methodologies that can be performed, it depends on the information required. The most popular one is the MRI that produce images of the sample for diagnostic and medical purposes.
In this section (*Introduction*) the main theory of NMR will be explained, then in the next section (*Materials and Methods*) an explanation of NMR apparata and techniques will be given.

1.1 NMR theory

The NMR phenomenon can be explained as an interaction between the *nuclear magnetic moment* $\vec{\mu}$ of nuclei and an external *magnetic fied* $\vec{B}_0$ which lead to an observable called *Magnetization* $\vec{M}$. In order to have information about the system, the magnetization must be perturbed by giving energy using radiofrequency pulses under the resonance condition. Then the restoring of equilibrium of $\vec{M}$ is measured and analyzed by a proper appartus. A brief explanation can be given as follow:

- An initial magnetic filed $\vec{B}_0$ is applied to the sample so the magnetic moments $\vec{\mu}$ are aligned respect to the $\vec{B}_0$ direction (parallel or anti-parallel), which results overall in the nuclear magnetization $\vec{M}$ of the sample
- A r.f. pulse is applied to the system in order to perturb the magnetization $\vec{M}$
- This perturbation creates a rotation around the initial magnetic field, where the evolution of the system is described by the motion equations
- The return to equilibrium creates a detectable electric signal which can be acquired and analyzed

Magnetization Now let's see more in detail the previous steps. The intensity of the acquired signal will be proportional to the spin $\vec{I}$ of the whole nucleus. It should be noticed that to have a non-zero I there are some conditions that must be satisfied: if both the mass number A and the atomic number Z

of the nucleus is even, then $I = 0$ so no NMR is possible; if the mass number A of the nucleus is even the atomic number Z of the nucleus is odd I is different from 0 so NMR is possible; if the mass number A of the nucleus is odd, then I is a fractional number and NMR is possible. At this point the magnetic moment can be written as:

$$\vec{\mu} = \gamma\hbar\vec{I} \tag{1}$$

where γ is the nucleus gyromagnetic ratio and it measures how strong an object can produce a magnetic moment due to spin. Because γ is very high for ^1H nuclei, from now on we will use values for ^1H-nucleus.
Now, since we are under the effect of magnetic field, from electrodynamics any magnetic moment will correspond to different energy states. Considering a magnetic field $\vec{B}_0$ along the z-axis the expression of the hamiltonian is:

$$H = -\vec{\mu}\cdot\vec{B}_0 = -\mu_z \cdot B_0 \tag{2}$$

Since for ^1H nucleus there is only a single proton, its values on z-axis are 1/2 and -1/2. The separation of Energy can be written as:

$$\Delta E = \frac{1}{2}\gamma\hbar B_0 - \frac{-1}{2}\gamma\hbar B_0 = \gamma\hbar B_0 \tag{3}$$

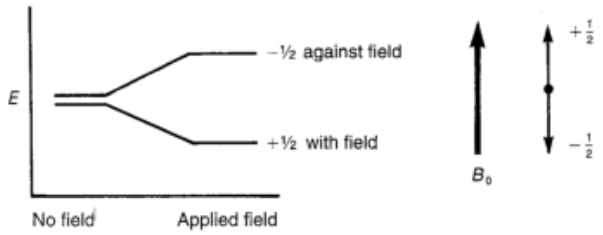

Figure 1. Energy levels splitting.

According to the Hamiltonian the aligned spins occupy a lower energy level or a higher energy level, as shown in Figure 1.
Now we can move from single nucleus framework to a multiple nuclei ones. In this case the overall magnetic moment of the sample $\vec{M}$ is the superposition of all the $\vec{\mu}_{nucleus}$. Since we know there are 2 distinct energy levels for each nuclear spin in ^1H nuclei, the equilibrium distribution of such states will follow a Boltzmann distribution. Moreover, the Curie Law, which states the linear proportionality between M and B_0 when $\hbar\gamma B_0 \ll 2KT$, allows us to write the magnetization at equilibrium as:

$$\vec{M} = N\frac{\gamma^2\hbar^2 I(I+1)}{3K_B T}B_0\hat{z} \tag{4}$$

where γ is the gyromagnetic ratio, I the spin of the nuclei, K_B is the Boltzmann's constant , T is the temperature and N is the total amount of nuclei per unit volume. Thus for hydrogen $I = 1/2$ so:

$$M = N\frac{\gamma^2\hbar^2}{4K_B T}B_0 \tag{5}$$

Perturbation In order to move the magnetization from the equilibrium a radio-frequency pulse is applied as an oscillating magnetic field $\vec{B}_1$ perpendicular to $\vec{B}_0$. The energy of the pulse in order to allow transitions from energy levels must be:

$$\Delta E = \hbar\omega_0 = \gamma\hbar B_0 \Rightarrow \omega_0 = \gamma B_0 \tag{6}$$

where ω_0 is called Larmor frequency, which is also the frequency of the oscillating $\vec{B}_1$ field (resonance condition).

Precession the Magnetization $\vec{M}$ will precess around the total magnetic field until it is aligned with it. The equations of motion for $\vec{M}$ and $\vec{B}_{TOT} = \vec{B}_0 + \vec{B}_1$ can be written as :

$$\frac{d\vec{M}}{dt} = \gamma(\vec{M}\times\vec{B}_{TOT}) \tag{7}$$

The movement of $\vec{M}$ will stop precession, when the angle between $\vec{M}$ and $\vec{B}_{TOT}$ are 0 and π (from the z-axis), corresponding to the equilibrium state alignments. The precession of $\vec{M}$ can be visualized and described using the laboratory frame and the rotating frame as shown in figure 2.

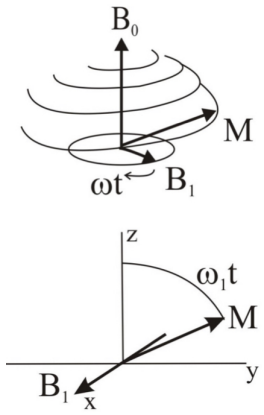

Figure 2. Precession seen respectively in the laboratory frame and rotating frame.

One important aspect is that, the change in direction is proportional to application time of the oscillating $\vec{B}_1$ field or as usually called RF-pulse, by an angle called *flip angle*:

$$\alpha = \gamma B_1 t_{pulse} \tag{8}$$

Usually the most common values for α are 90° and 180°, meaning respectively a $\vec{M}$ on the transverse plane (x-y plane) and on the opposite side of the z-direction.

FID The return of the $\vec{M}$ to equilibrium corresponds to a change in magnetic field on the x-y plane, inducing a current in the detector. The frequency of the signal is the larmor frequency ω_0 due to the precession of $\vec{M}$. The acquired signal is called Free Induction Decay or FID (because $\vec{M}$ precesses dumping to zero with an exponential decay as shown in Figure 3).

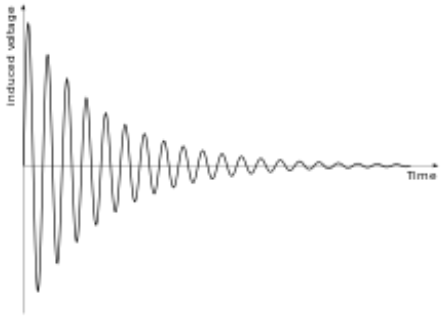

Figure 3. Free Induction Decay.

1.2 Relaxation

The decay of RF-induced NMR spin polarization is characterized in terms of two separate processes, each with their own time constants called T_1 and T_2. As a matter of fact, we can see the $\vec{M}$ along the z-direction and on the the transverse plane (x-y plane).
Now if we consider $t = 0$ the moment when the RF-pulse is cancelled and the acquisition can start, the magnetization $\vec{M}(0)$ is already tilted. Due to equilibrium statistics we know that:

$$M_z(t \to \infty) = N\frac{\gamma^2\hbar^2}{4K_BT}B_0 \qquad M_{xy}(t \to \infty) = 0$$

Using the Bloch equations to describe the evolution along these two directions [1]:

$$\frac{dM_z(t)}{dt} = -\frac{(M_z(t) - M_0)}{T_1} \tag{9}$$

$$\frac{dM_{xy}(t)}{dt} = -\frac{M_{xy}(t)}{T_2} \tag{10}$$

where M_0 is the steady state nuclear magnetization, that is for example when $t \to \infty$. The equations are separable and the solutions are:

$$M_z(t) = M_z(0)\mathrm{e}^{-t/T_1} + M_0(1 - \mathrm{e}^{-t/T_1}) \tag{11}$$

$$M_{xy}(t) = M_{xy}(0)\mathrm{e}^{-t/T_2} \tag{12}$$

where T_1 and T_2 are the characteristic relaxation parameters and they basically describe how fast the relaxation of M_z and M_{xy} occurs. Smaller the values, faster the relaxation. If you look at the solution for $M_z(t)$, you can notice the $M_z(0)$ term, which is is not but the value on the z-axis of $\vec{M}(0)$. As said previously, the position of $\vec{M}$ depends on the *flip angle* $\alpha = \gamma B_1 t_{pulse}$. Therefore for particular and most common cases, thus for $\alpha = 90°$ and $\alpha = 180°$ we can modify the Eq.11 in order to have:

$$M_z(t) = \begin{cases} M_0(1 - \mathrm{e}^{-t/T_1}) & \text{if } \alpha = 90° \\ M_0(1 - 2\mathrm{e}^{-t/T_1}) & \text{if } \alpha = 180° \end{cases}$$

As regard M_{xy}, the component of magnetization in x-y plane decays exponentially and reaches its equilibrium value at zero. The main mechanism of this process is the dephasing of individual nuclei magnetization vector $\vec{\mu}_{nuc}$ therefore T_2 is a measure of this dephasing. In an idealized system, all nuclei in a given chemical environment, in a magnetic field, precess with the same frequency. However this is only ideal because the applied $\vec{B}_0$ field is not severely uniform, thus each nucleus will have a slightly different rotating frequency resulting the M_{xy} will dephase even faster because of the inhomogeneities. For this reason the T_2 parameter will be labelled as T_2^*. A summary of this process is shown un Figure 4.

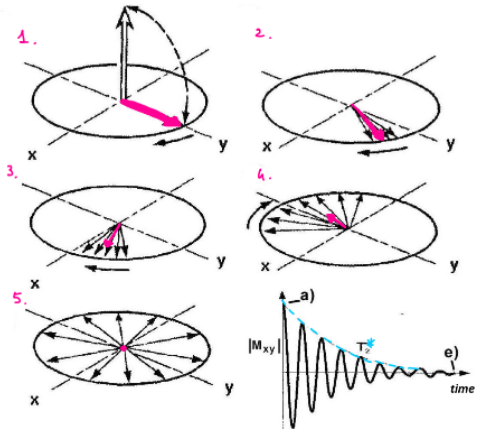

Figure 4. Depahsing of the Magnetization on the x-y plane and the acquired FID. Note that the relaxation time costant of the FID is the T_2^*.

Anyway there are methods that allow to overcome the inhomogeneities and get the T_2 relaxation constant. One consist in the application of a second pulse of 180°. This is called *Spin-echo sequence*. As shown in Figure 5, it is possible to get the T_2 thanks to the so called *echo*.
To conclude about relaxation, it should be noticed that in general $T_2 \leq T_1$ due to the fact that T_2 is an entropic process while T_1 is an energetic process.

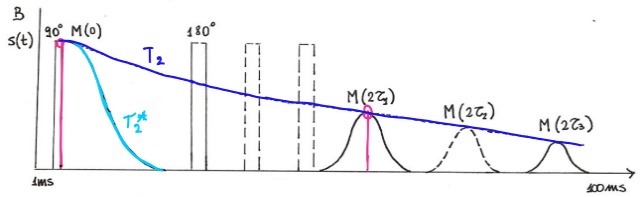

Figure 5. Spin-echo sequence sketch. In light-blue the T_2^* relaxation constant, in dark-blue the T_2 ones.

1.3 Diffusion

Diffusion is the net movement of anything (could be molecules, atoms, ions) from a region of higher concentration to a region of lower concentration. This process is subject by random motion due to random fluctuations. Diffusion can be analyzed by NMR because it lowers the NMR signal.The main method of

[1] doing some assumptions like being in the rotating frame

this process is that, the interaction between dipoles create additional magnetic field to the $\vec{B}_0$ field, creating additional non-uniformity in the local magnetic field. This non-uniformity leads to a dephasing in the individual $\vec{\mu}_{nucl}$. In Figure 6 it can be seen how diffusion can affect the dephasing of M_{xy} resulting in a lowered signal.

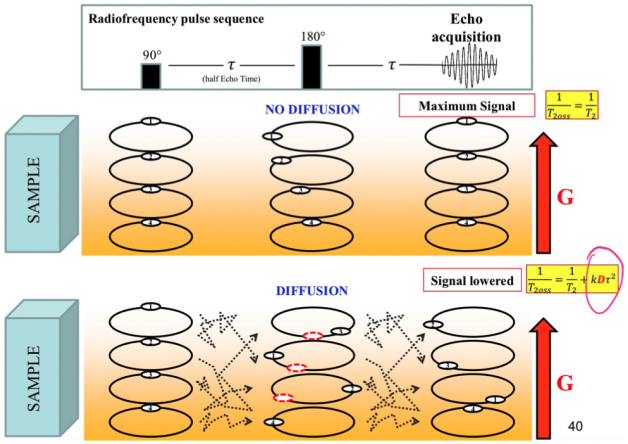

Figure 6. Diffusion affecting the dephasing of M_{xy}.

The CPMG sequence should allow one to obtain relaxation curves not affected by diffusion, assuming a short half-echo time τ. It is possible to demonstrate that in the presence of a constant gradient g:

$$R_2^{obs}(\tau^2) = \frac{1}{T_2^{obs}(\tau^2)} = \frac{1}{T_2} + \frac{1}{3}\gamma^2 g^2 D\tau^2 \tag{13}$$

where τ is half echo time, D the diffusion constant, and g the magnetic gradient. However this is valid when diffusion has no restrictions, thus is free. In case of a restricted geometry, most common sequences are based on pulsed field gradient, that consists in applying two gradients separated by a diffusion time Δ and the displacement along the z-coordinates will become a function of the diffusion time Δ, D and the restricting space. In particular we can define:

$$\xi = \frac{D\Delta}{R^2} \tag{14}$$

where Δ is the diffusion time and R is the radius of the restricting volume. In two dimensions, as it can be seen in Figure 7, if $\xi << 1$ the particles do not spread enough to be confined and so the intrinsic diffusion coefficient is obtained; if $\xi \simeq 1$ a fraction of the particles will be affected by the restricted geometry and it will be observed an apparent diffusion coefficient D_{app} that will depend on Δ; if $\xi >> 1$ the apparent diffusion is much lower than the true diffusion value since the area is very small compared to the diffusion capabilities of the particles.

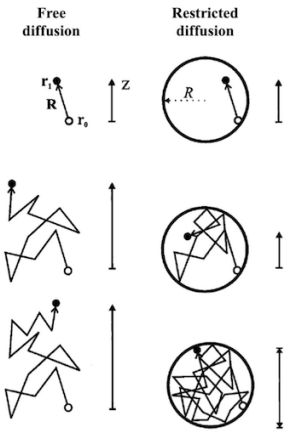

Figure 7. Sketch of free diffusion vs restricted diffusion.

2. Materials and Methods

In the first part (*Materials*) of this section both homogeneous magnetic field and single-sided NMR apparata will be described. Then, in the second part (*Methods*) the various sequences and procedures exploited for the lab sessions will be described.

2.1 Materials

In order to exploit the physical phenomenon of the Nuclear Magnetic Resonance and to study there are many devices, each one with specific features to accomplish different investigations. Conventional NMR apparata work with homogeneous magnetic field and because of their sizes they are not easy to move. Moreover, they require a proper cooling system in order to refrigerate the coils. Single-sided NMR apparata instead, such as NMR-MOUSE (Margritek, Germany), work with inhomogeneous field, furthermore they are portable devices which allow one to perform non-destructive and non-invasive measurements directly in-situ.

2.1.1 JEOL Electromagnet

The Electromagnet Jeol C-60 is a in-house relaxometer based on an electromagnet controlled by the PC-NMR portable console (Stelar, Pavia). The magnetic field can be varied in the range 0.05 T - 1 T. The Jeol apparatus offers a good homogeneous magnetic field but with a significantly small sensitive volume. In fact, the object of analysis must be sampled and placed in a glass pipe before going underneath the magnetic filed. In Figure 8 it is shown a schematic of the JOEL electromagnet. As one can see from the schematic, the current flowing into the main coils (in red) produce an horizontal homogeneous magnetic field $\vec{B}_0$, while the oscillating $\vec{B}_1$ field is obtained by a transmitter-receiver probe. Note that a lock system is attendant in order to secure the frequency of the magnetic field $\vec{B}_0$ changing, eventually, the flowing current. Before one can perform the analyses, very important operations are the matching and tuning of the probe.The former consist in matching the standard 50 Ohm output changing

the impedance (adjusting the capacitance) of the circuits, in order to maximaze the acquired signal. The latter consist in centering the resonance frequency (20 MHz for a magnetic field of 0.5 T) in order to send the correct rf pulse.

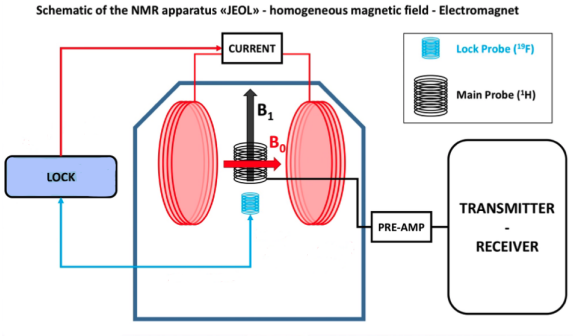

Figure 8. Schematic of the Joel Electromagnet.

2.1.2 Single-Sided: NMR-MOUSE PM10

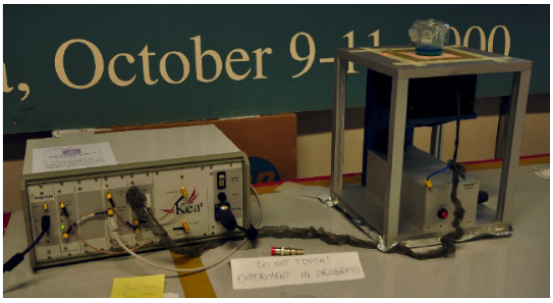

Figure 9. Single Sided NMR-MOUSE PM10 (right) and the KEAII spectrometer (left).

Single sided NMR devices, or sometimes Unilateral NMR, are compact, portable and designed for in-situ measurements. The necessity of in-situ measurements made the dimensions of magnets to be drastically reduced, thus the strength and the homogeneity of the field is lowered respect to the conventional NMR instruments. They started to be commercialized as well-logging instruments and become much more widespread in the mid of the 90's after the development of the NMR-MOUSE (MObile Universal Surface Explorer) which was tested to be useful for material quality screenings. Unilateral NMR magnets are characterized by inhomogeneous field and a strong magnetic gradient, $g = \frac{\Delta B_z}{\Delta y}$, in the y direction, perpendicular to the magnet surface. The radio-frequency coil that generates the pulse and acquire the signal (the coil is a transceiver) is located between the magnetic poles of a U-shaped magnet, as shown in Figure 10.

The peculiarity of this kind of apparatus are the really compact dimensions that make it suitable for analyzing a great variety of subjects especially in the Cultural heritage field. Moreover some kind of apparatus such as the NMR-MOUSE own the possibility of shifting the sensitive volume inside the analyzed object thanks to the high-precision automated lift,

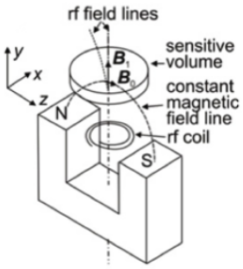

Figure 10. Sketch of a U-shaped NMR magnet.

piloted by a proper software, that allows steps of micrometers as shown in Figure 11. In this way it is possible to obtain profiles of the sample with maximum depth of the order of centimeters. This is really useful when someone wants to investigate the properties of the object not only on the surface but also in depth in a non destructive way.

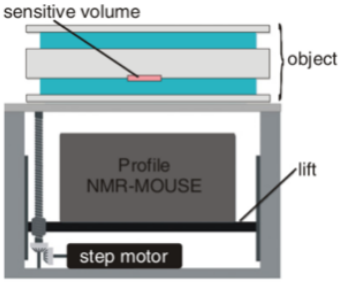

Figure 11. Schematic of NMR-MOUSE. Please note the difference between the object and the sensitive volume.

The instruments are controlled, usually by a spectrometer (like the KEAII) connected by a PC and managed by a proprietary software (Prospa, Magritek). As regard the NMR-MOUSE PM10, the Magnetic Field in the sensitive volume is $B = 0.327$ T for ^1H nuclei of Larmor frequency $\nu = 13.9$ MHz. It could be noted that the position between permanent magnet and sensitive volume is fixed, and in the case of the NMR-MOUSE PM10 is at 10 mm from the surface of the magnet. Moreover it is equipped with spacers, each of them has 2 mm of thickness, that can be insert or removed, between the permanent magnet and RF-coil in order to reduce the distance between the coil and the sensitive volume. The smaller is the distance, between the coil and the sensitive volume, greater will be the SNR. On the other hand, the smaller is the distance, the smaller is the maximum depth achievable inside the sample. In fact, as shown in Figure 12, the thickness of the sensitive volume is related to the frequency band as: $\Delta y_{\text{th}} = \frac{\gamma \Delta \omega}{g}$, where $\Delta\omega \propto \frac{1}{t_{\text{pulse}}}$. This means that the distance between the sensitive volume and the coil can also affect the thickness of the sensitive volume. So the choice of the spacer configuration is fundamental to achieve the best signal-to-noise ratio performance for the experiment depending on the maximum depth to analyze.

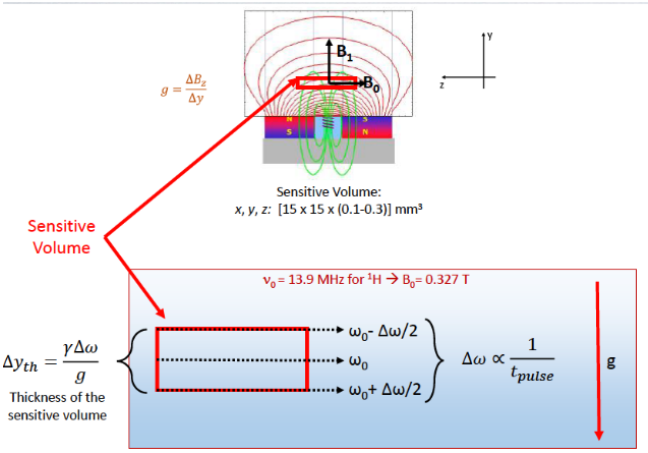

Figure 12. Thickness of the sensitive volume depending on the bandwidth.

2.2 Methods

This part of the report is aimed to show the main Methods used to perform the experiments and to acquire the data. Methods include the Free Induction Decay (FID), Spin-Echo, Carr-Purcell-Meiboom-Gill (CPMG), inversion recovery sequence and the UPEN algorithm.

2.2.1 Free Induction Decay

As described in the *Introduction* section, the Free Induction Decay (FID) is the is the observable NMR signal generated by non-equilibrium nuclear spin magnetization precessing about the magnetic field. The acquisition of the FID is obtained after a RF-pulse (usually 90°) and, after a repetition time TR, the process is repeated and another FID can be acquired. A simple schematic is shown in Figure 13. Note that the signal is acquired after a very short time called dead time in which the system is not sending either acquiring signals. As you can see the FID signal decays exponentially towards zero with a relaxation constant T_2^*. Note that the signal is not shown as a dumping one because it is represented in the rotating frame so in a resonance domain, otherwise the shape is like the one showed in Figure 3.

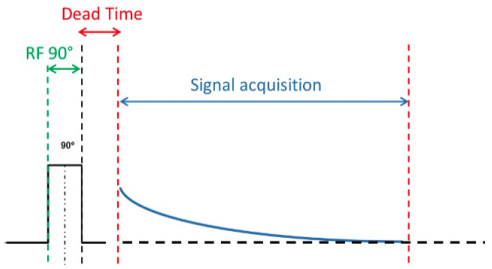

Figure 13. Schematic of the FID acquisition.

2.2.2 Spin-Echo sequence

The Spin-Echo sequence, as shown in Figure 14, consists in a first 90°-pulse followed by a second 180°-pulse applied after a certain interval of time (T_E/2). The echo time (T_E) represents the time from the center of the first RF-pulse to the center of the echo. The 180° pulse, produces an echo due to the re-phasing of the spins. The echo envelope give us the correct exponential T_2 relaxation process (Figure 5). In fact, the exponential relaxation T_2^* measured on the FID would have been shorter. The decay of the magnetization as function of the T_E is given by the equation:

$$M_{xy}(T_E) = M_0 e^{-\frac{T_E}{T_2}} \tag{15}$$

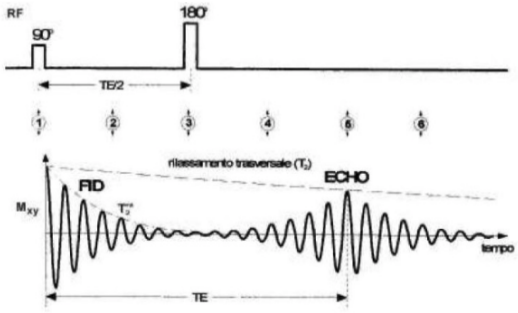

Figure 14. Sketch of the Spin-Echo sequence.

2.2.3 CPMG sequence

Carr-Purcell-Meiboom-Gill (CPMG) pulse sequence for measuring T_2, as shown in Figure 15 consists in a first 90°-pulse followed by a first 180°-pulse after $T_E/2$ and a train of 180°-pulse interspersed by the echo-time (T_E) in order to obtain several echoes. The echo train reduces the effect of diffusion on the acquired signal. The train echo envelope give us the exponential T_2 relaxation process (assuming no constant magnetic field gradient):

$$M_{xy}(t) = M_0 e^{-\frac{t}{T_2}} \tag{16}$$

In case of a constant magnetic field gradient g, such as in the case of a Single Sided apparatus, for a CPMG sequence, the acquired signal amplitude can be expressed as:

$$A(t) = A(0) e^{-\frac{t}{T_2} - \frac{1}{3}\gamma^2 g^2 D \tau^2 t} = A(0) e^{-\frac{t}{T_2^{obs}}} \tag{17}$$

where the T_2^{obs} parameter is the observed relaxation time T_2 in the presence of diffusion, which differs from the T_2^{bulk} so in the case no diffusion takes place. Therefore, Eq. 13 is true. This is very helpful in order to measure self-diffusion coefficient. The problem is that we don't measure directly T_2^{obs} but the signal decay which acts, in principle, as a mono-exponential, even if in reality several exponentially decaying components are present in the acquired signal.

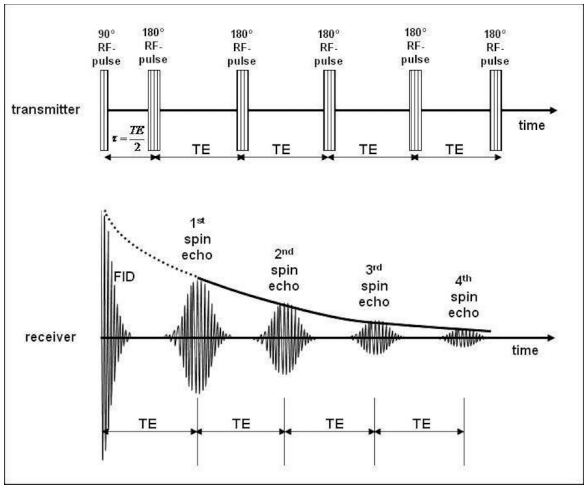

Figure 15. Sketch of the CPMG sequence.

2.2.4 Inversion Recovery sequence

The inversion recovery (IR) pulse sequence for measuring T_1, as shown in Figure 16 consists in a first 180° inverting pulse and a 90°-pulse . The time between the 180° inverting pulse and the 90°-pulse is called the inversion time (τ or T_I). The evolution of the magnetization is given by:

$$M_z(\tau) = M_0(1 - 2e^{-\frac{\tau}{T_1}}) \tag{18}$$

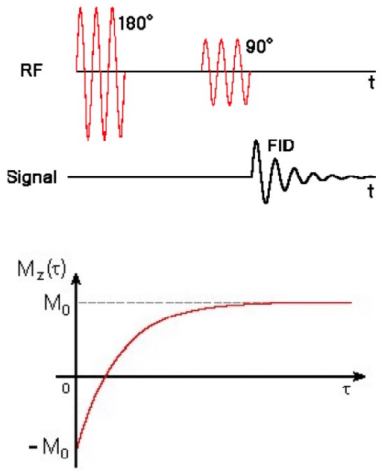

Figure 16. Sketch of the IR sequence.

2.2.5 UPEN

The NMR relaxation processes are manifested as decaying signals over the acquisition time. NMR relaxometry data analysis involves a Laplace inversion to obtain a distribution of relaxation times starting from the acquired NMR signals. Depending on the nature of the sample, the relaxation assumes a proper behavior which is related to the complexity of the system. Just for pure/bulk materials the spins are in the same environment and the relaxation can be described by a mono-exponential function. However, in the most of real systems, the relaxation is described by a multi-exponential behavior. Assuming to have a system composed of a discrete number $M > 2$ of components, then the signal $S(t)$ can fit the model:

$$S(t_i) = \sum_{k=1}^{M} a_k e^{-\frac{t_i}{T_{1,2}\,k}} \tag{19}$$

Since the fit of a discrete distribution of systems with more than two components has about the same error as the fit of a continuous distribution, a continuous distribution of relaxation times can be considered. In our case the Laplace transform:

$$f(x) \to F(z) = \int_0^\infty f(x) e^{-zx} dz \tag{20}$$

can be written as:

$$S(t) = \int_0^\infty f(T_{1,2}) e^{-\frac{t}{T_{1,2}}} dT_{1,2} \tag{21}$$

where $f(T_{1,2})$ is the density signal function and $S(t)$ is the acquired NMR Signal. One should invert the signal from the measured time scale t to the one of the relaxation times $T_{1,2}$ in order to obtain the function $f(T_{1,2})$. This mathematical operation is called Inverse Laplace Transform from the measured time scale "t" to the one of the relaxation times.
Mathematically, the inversion is an ill-conditioned problem, because $S(t)$ is not an analytical function but it is given by experimental points affected by noise that gives an infinite number of solution that satisfy the inversion. To overcome this difficult it is hypothesized that the signal is composed by a high number of exponential components (order of 10^2) and then the so-called quasi-continuous distribution of relaxation times is computed in order to find a unique solution. The procedure is made by algorithms which can have different approaches. The most common approach imposes to minimize a target function. In the inversion algorithms a smoothing coefficient , which is generally fixed, is used to avoid abrupt variations in the distribution. Anyway some algorithms might wide the narrow peak and break the tail of the distribution curve into several peaks that could be falsely interpreted as separate populations, that not well-represents the real system. Among the various algorithms, UPEN(Uniform PENalty), developed in Bologna, introduces the same "penalty" in the data along the entire distribution curve, avoiding peaks not justified by the data. The algorithm works by using a target function with a smoothing coefficient variable along all the points of the computed distribution function, avoiding the creation of peaks maybe not justified by the data, as shown in Figure 17.

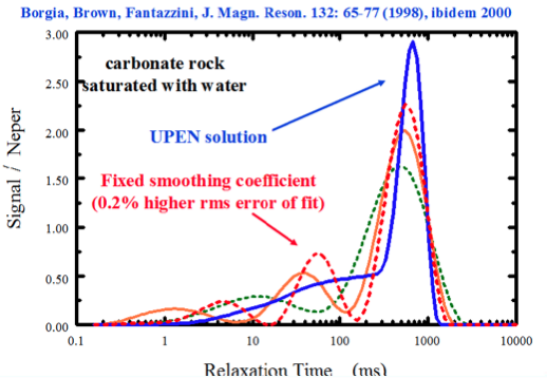

Figure 17. Comparison between inversion algorithms and UPEN.

3. Results and Discussion

This part of the report is aimed to show and to discuss the results of the experiments performed during the lab experiences. In particular FID acquisition, T_1 and T_2 relaxation measurements, Self-Diffusion Coefficient measurements and CPMG measurements on porous medium.

3.1 FID Acquisition

As regard the FID, the acquisition was performed using the Joel-C60 , thus in an homogeneous magnetic field and as sample a small piece of natural rubber placed in a glass pipe. After the matching and tuning process the FID was acquired as shown in Figure 18 where you can notice how fast the decay of the magnetization occurs since it is characterized by the T_2^* constant, as explained previously. However, depending on the pulse length t_{pulse} we can have different flip angles ($\alpha = \gamma B_1 t_{pulse}$) resulting in FID characterized by a different initial amplitude, as shown in Figure 19. This was investigated performed several FID acquisitions to investigate the max value of the initial amplitude varying the pulse length from 0 to 20 μs. The result is shown in Figure 20 where you can see the that the max value of the amplitude is obtained for $t_{pulse} = 3.5\mu s$ corresponding to $\alpha = 90°$ so when the magnetization is completely flipped on the transverse plane. Note that for $\alpha = 180°$ the signal amplitude is zero, this is because the signal is measured on the x-y plane so when we flip the magnetization on the z axis in the opposite direction, the value of the measured amplitude on the x-y plane is zero.

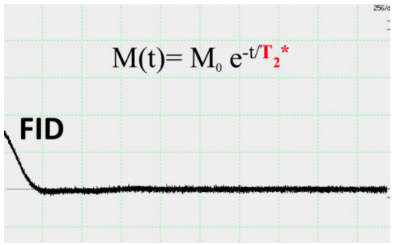

Figure 18. FID evolution. Note how fast the magnetization decays.

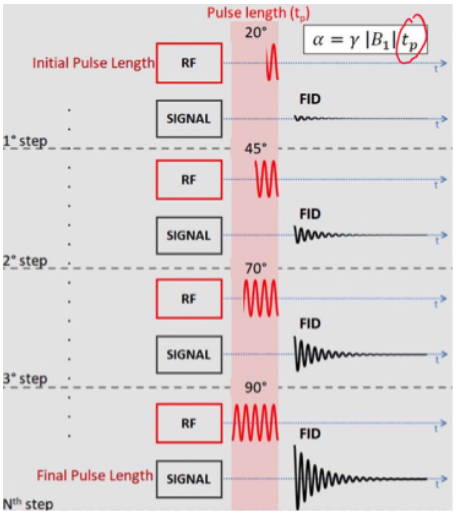

Figure 19. FID shape depending on the flip angle α.

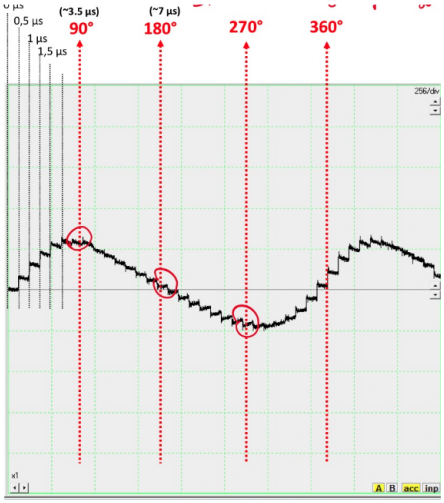

Figure 20. Repetition of 40 FIDs varying the pulse length.

3.2 T2 Measurements

In order to measure the T_2 time constant, Spin-Echo and CPMG sequences were used. In this case the sample was made of Doped Water (EDTA H_2O). As regard the Spin-Echo, multiple acquisitions were made varying T_E since, dealing with an homogeneous B_0, the relation of the amplitude of the echo as function of T_E is given by:

$$A(T_E) = A(0)\mathrm{e}^{-\frac{T_E}{T_2}} \tag{22}$$

In Figure 21 you can see the fit of the acquired data. The function used to fit the data in this case was the Eq. 22 since the field generated by the Joel-C60 is homogeneous. In general, in presence of a magnetic field gradient g, the previous relation is not true because the effect of diffusion dominates the evolution of the signal, so the Eq. 22 becomes in a more general form:

$$A(T_E) = A(0)\mathrm{e}^{-\frac{T_E}{T_2} - \frac{2}{3}\gamma^2 g^2 D(T_E/2)^3} \tag{23}$$

One drawback of the Spin-Echo sequence is that you need to start the sequence from the beginning again and again changing the echo time, which is a quite long process. In this case, the CPMG sequence is more advantageous since we have a train of 180° pulses all separated by T_E so the acquisition time is in the order of echo time which is much less compared to repetition time. Another advantage is that CPMG sequence is very handy when it comes to measure the diffusion of particles inside the sample thanks to the minimization of echo time. In fact, the minimization lowers the effect of diffusion, leading to obtaining a T_2 value similar to non-diffusive sample. In Figure 22, you can see the difference between a FID acquisition and a CPMG one. Please note the difference between the T_2^* and the T_2 decay of the magnetization. As you can see the T_2^* is much faster than the T_2.In fact, the FID after 3 ms is already decayed, while the CPMG signal after 30 ms is still decaying.

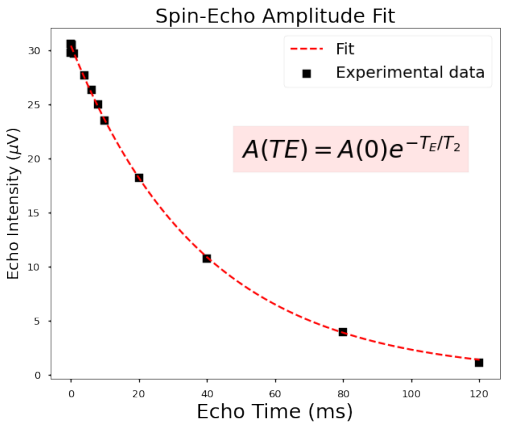

Figure 21. Spin-Echo Amplitude Fit.

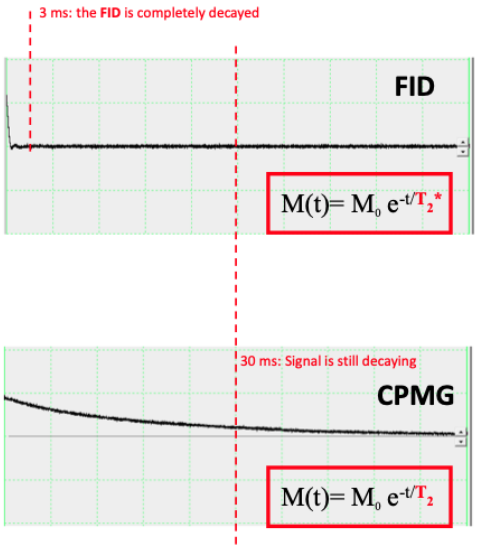

Figure 22. Comparison between the FID and CPMG signals.

3.3 T1 Measurements

As regard the T_1, as explained previously, it is related to the relaxation process of the longitudinal component of the magnetization. However, in NMR experiments, we can only measure the magnetization component in the transverse plane (x-y plane) because the signal is generated by the precession of the magnetization in that plane. Thus, in order to get information about the evolution of $M_z(t)$, the inversion recovery sequence was performed, varying time interval τ or TI between the two RF pulses. In Figure 23, you can see in semi-log scale an IR sequence sampling. Note that varying τ the acquired signal is not but the FID. The value of the magnetization M_0 can be extrapolated, fitting each FID by an exponential function and storing the value of the amplitude at $t = 0$, as shown in Figure 24 both in semi-log and linear scale.

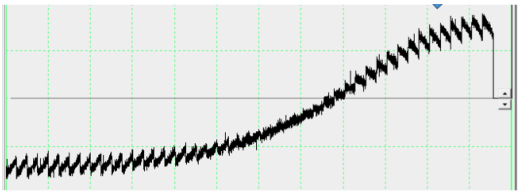

Figure 23. IR sampling in semi-log scale.

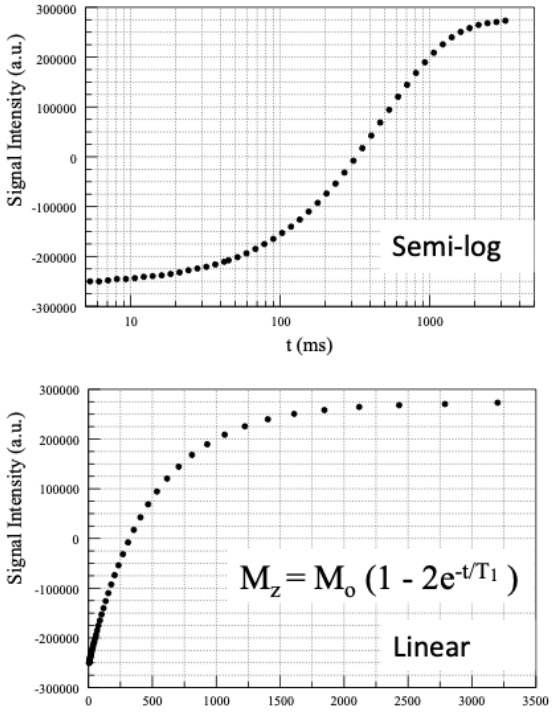

Figure 24. Inversion recovery sequence in Semi-log (up) and Linear (bottom) scale.

3.4 Self-Diffusion Coefficient Measurements

The measurements of the Self-Diffusion Coefficient D was done using T_2^{obs} data acquired using the NMR-MOUSE PM10 (so local magnetic field gradient) and CPMG sequences varying τ for EDTA - H_2O (Doped Water), Soltrol 130 and Soltrol 170 which are paraffin hydrocarbon more viscous than water. For these measurements the setup consisted in the NMR-MOUSE PM10 with all the spacer inserted reducing the distance from the sensitive volume since we were not interested in depth profiling, thus maximizing the SNR. For all the substances, the CPMG sequence specifications are reported in Figure 25. After the data acquisition the signals have been inverted by UPEN to get the T_2^{obs} distributions for each half-echo time τ.

Sample	τ (μs)	90° pulse length (μs)	TR (s)	# echoes	# scans
Water	25	4	1	8000	400
	35	4	1	8000	400
	50	4	1	6000	400
	75	4	1	2000	600
	100	4	1	1000	400
	175	4	1	800	400
Soltrol 130	20	8.4	6	8000	100
	25	8.4	6	8000	100
	30	8.4	6	8000	100
	30	8.4	6	8000	100
	50	8.4	6	8000	100
	70	8.4	6	8000	100
	90	8.4	6	8000	100
	100	8.4	6	8000	100
Soltrol 170	25	4	3.5	8000	600
	50	4	3.5	8000	600
	75	4	3.5	8000	600
	100	4	3.5	4000	600
	125	4	3.5	2000	600
	150	4	3.5	1000	600

Figure 25. CPMG parameters.

As you can see on the left side of Figure 29, in which the distribution of T_2^{obs} for different τ (obtained from UPEN inversion) are shown, as τ increases the value of the T_2^{obs} decreases. This is true since from Eq. 13 $1/T_2^{obs}$ is proportional to D and τ^2, assuming of course a gradient g which in this case was $g = 17\ T/m$. Moreover, you can notice that not only the value of the T_2^{obs} decreases but also the signal density. In fact, as shown in Eq. 17 the decreasing in signal amplitude is also proportional to D and τ^2. This can be seen on the right side of Figure 29, where the slope of the mono-exponential fit (by UPEN) is also decreasing (note that the NMR Signal is in log scale). Last but not least you can also notice that the peaks for higher values of τ have a wider Full Width at Half Maximum (FWHM) denoting an higher dispersion of the data, thus a change in the resonance frequencies due to the inhomogeneities, as explained in the *Diffusion* subsection. In order to quantify the Self-Diffusion coefficient for each of the three substances, we fitted the data with a linear function, as shown in Figure 26, exploiting the Eq.13. Therefore to evaluate D we used the following relation:

$$D = \frac{3 \cdot Slope}{\gamma^2 g^2} \qquad T_2 = \frac{1}{Intercept}$$

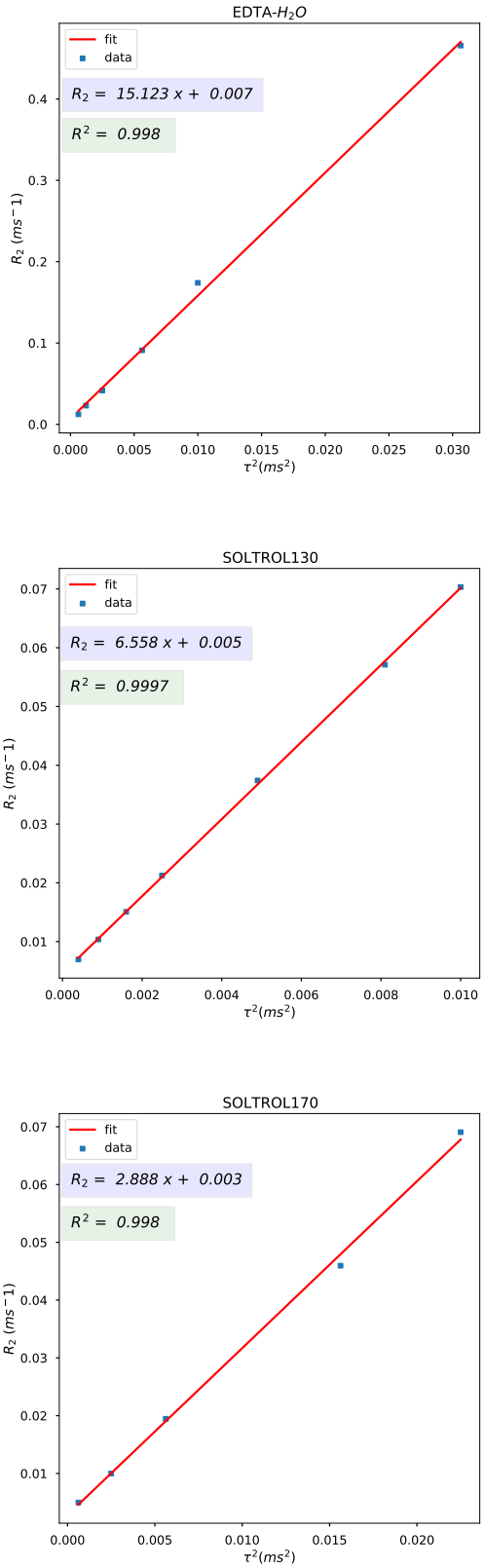

Figure 26. R_2^{obs} fit for EDTA-H_2O Soltro130 and Soltrol170.

The parameters obtained from the fit for each substance are shown in Table 1 with the errors from the linear fit.

Substance	Slope	Intercept
Water:	15.123 ±0.341	0.007 ±0.005
Soltrol130:	6.558 ±0.049	0.005 ±0.0003
Soltrol170:	2.888 ±0.074	0.003 ±0.001

Table 1. Table of obtained parameters from the linear fit.

Doing some algebra, the measured Self-Diffusion coefficients are reported in Table 2. As you can see the measured values are higher than the ones obtained from literature, especially from Soltrol130. The reason of these high deviation from the literature values could be due to different reasons. First of all, the errors are obtained from the linear fit so they not represents the real experiment error. In fact, as you can see the fit error for Soltrol130 is one of the lowest but the deviation from the literature value is the highest. Moreover, R_2^{obs} is obtained using only the T_2^{obs} peak values instead other values could have been used (i.e. a value between the peak and the geometrical mean). Finally, an important parameter that has not been taken into account is the temperature T since diffusion is a function of the temperature, increasing when T increases. In fact, performing the experiment one should be mindful of the environmental temperature but especially of the temperature of the RF-coil since it could overheating because of the power for generating RF-pulse and/or the time of application (especially for CPMG sequence where a train of 180-pulse are performed) thus heat the sample especially if directly in contact with the surface of the apparatus.
Last thing to note is that we estimated D using a Eq.13, assuming no restricted geometry so ξ to be less than 1 and so that the estimated D_{app} coincides the true D which is not always true as explained in the *Diffusion* subsection.

Substance	$D_{lit}(\frac{\mu m^2}{ms})$	$D_{measured}(\frac{\mu m^2}{ms})$	dev $(\frac{\mu m^2}{ms})$
Water:	2.14	2.19 ±0.05	0.05
Soltrol130:	0.728	0.951 ±0.007	0.223
Soltrol170:	0.401	0.419 ±0.001	0.018

Table 2. Table of Self-Diffusion coefficients.

3.5 CPMG on porous medium

Measurements of relaxation times give us information about fluids, pores space and their interaction with the porous medium. This is possible exploiting the so-called "Surface Effect" which describes the interaction between the solid surface of the porous matrix and the molecular fluid in contact with it. The measured relaxation times of hydrogenated fluid confined into a porous medium are correlated to the Surface/Volume (S/V) ratio of the restricting geometries. If we consider a fully saturated pore of volume V and the surface of the pore S, the relaxation times can be described as:

$$\frac{1}{T_{1,2}^{obs}} = \rho_{1,2}\frac{S}{V} + \frac{1}{T_{1,2}b} \tag{24}$$

where $\rho_{1,2}$ is the surface relaxivity and the indexes b denotes the bulk relaxation (for not confined fluid).
The distribution of the relaxation times indicates the distribution of the pore sizes in which the fluid is confined.
In the presence of a magnetic field gradient g, such as the case of the NMR-MOUSE, molecular diffusion must be accounted for. As a consequence, in strongly inhomogeneous field, the transverse relaxation rate also depends on the g strength:

$$\frac{1}{T_2^{obs}} = \rho_2\frac{S}{V} + \frac{1}{T_2 b} + \frac{D(\gamma g T_E)^2}{12} \tag{25}$$

where D is the diffusion coefficient, γ is the gyromagnetic ratio of the observed nucleus, and T_E is the echo time. In the case of single-sided NMR devices, the gradient g is particularly strong. Thus, the effect of the gradient can prevail the "Surface effect" especially for the ^1H in the biggest pores.
We can exploit the Surface Effect to discuss the results about the the distribution of T_2^{obs} for bulk water and a porous medium such as Vicenza stone saturated with water obtained from CPMG sequence, shown in Figure 27. As you can see, there is a difference between the two distributions even if the signal is obtained for the same hydrogenated fluid (Water). In bulk water the peak of T_2^{obs} is a broad narrow one without tails, thus corresponding to the $T_2 b$, while for Vicenza Stone there is a peak for higher T_2 values and a very broad peak for shorter ones. Qualitatively, this can be interpreted as the presence of two exponential-decay components, one which relaxes slower, related to bigger pores and one which relaxes faster related to smaller pores. As a matter of fact, this is represented in Figure 28 in which for the Vicenza stone the decaying in semi-log scale is not linear but exponential, while for bulk water the trend is linear denoting a mono-exponential behaviour.
An interesting comparison could have been done measuring also the T_1 relaxation constant in order to assert that diffusion doesn't prevail over the surface effect, making lose crucial information about S/V ratio, and/or to get T_1 T_2 correlation maps.

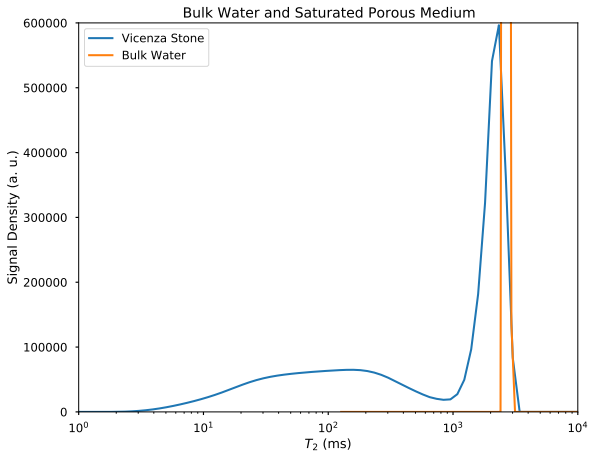

Figure 27. T_2^{obs} distribution obtained by UPEN for Bulk Water and saturated Vicenza Stone.

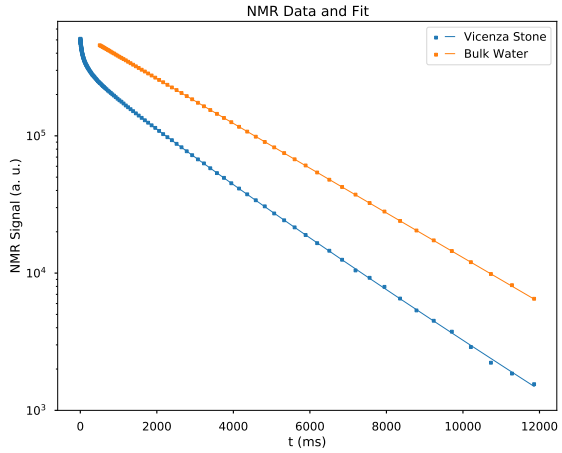

Figure 28. NMR signal and fit obtained by UPEN for Bulk Water and saturated Vicenza Stone.

4. Conclusion

Finally we can say that the lab experiences enabled us to become familiar with the principles, apparata and sequences used in NMR and also to quantify the diffusion coefficient for different substances with single sided NMR MOUSE.
The first part was aimed to learn the basic concepts, in particular, the NMR phenomenon, Relaxation and Diffusion.
Then, Materials and Methods have been described. Regarding the Apparata, both homogeneous and inhomogeneous magnetic field apparata have been described, focusing respectively on JOEL-C60 and Single-Sided NMR-MOUSE PM10. Regarding Methods, the FID, the Pulse sequences used for the measurements such as Spin-Echo, CPMG and Inversion Recovery have been treated. Moreover, a brief explanation on the UPEN inversion Algorithm has been given.
The last but not least part was aimed to show the result of all the lab measurements. Firstly, a brief overview on the FID acquisition and the pulse length importance has been done. Then, the measurements of T_2 and T_1 in homogeneous magnetic field. Finally, exploiting the inhomogeneous magnetic field of the NMR-MOUSE PM10, the self diffusion coefficient for Water, Soltrol130 and Soltrol 170 has been determined and CPMG measurments on bulk water and porous medium have been discussed.

References

[1] Filitto, G., Testa, C., and Brizi, L., "Alma Mater Studiorum - Tesi di Laurea Triennale" *Magnetic Resonance for fluids in porous media: applications to Cultural Heritage*, June 2019.

[2] Barbieri, M., Brizi, L. *Use of Mobile Single-Sided NMR for the Diagnosis of Osteoporosis: a Preliminary Study.*", 2017

[3] https://en.wikipedia.org/wiki/Nuclear_magnetic_resonance

[4] https://en.wikipedia.org/wiki/Relaxation_(NMR)

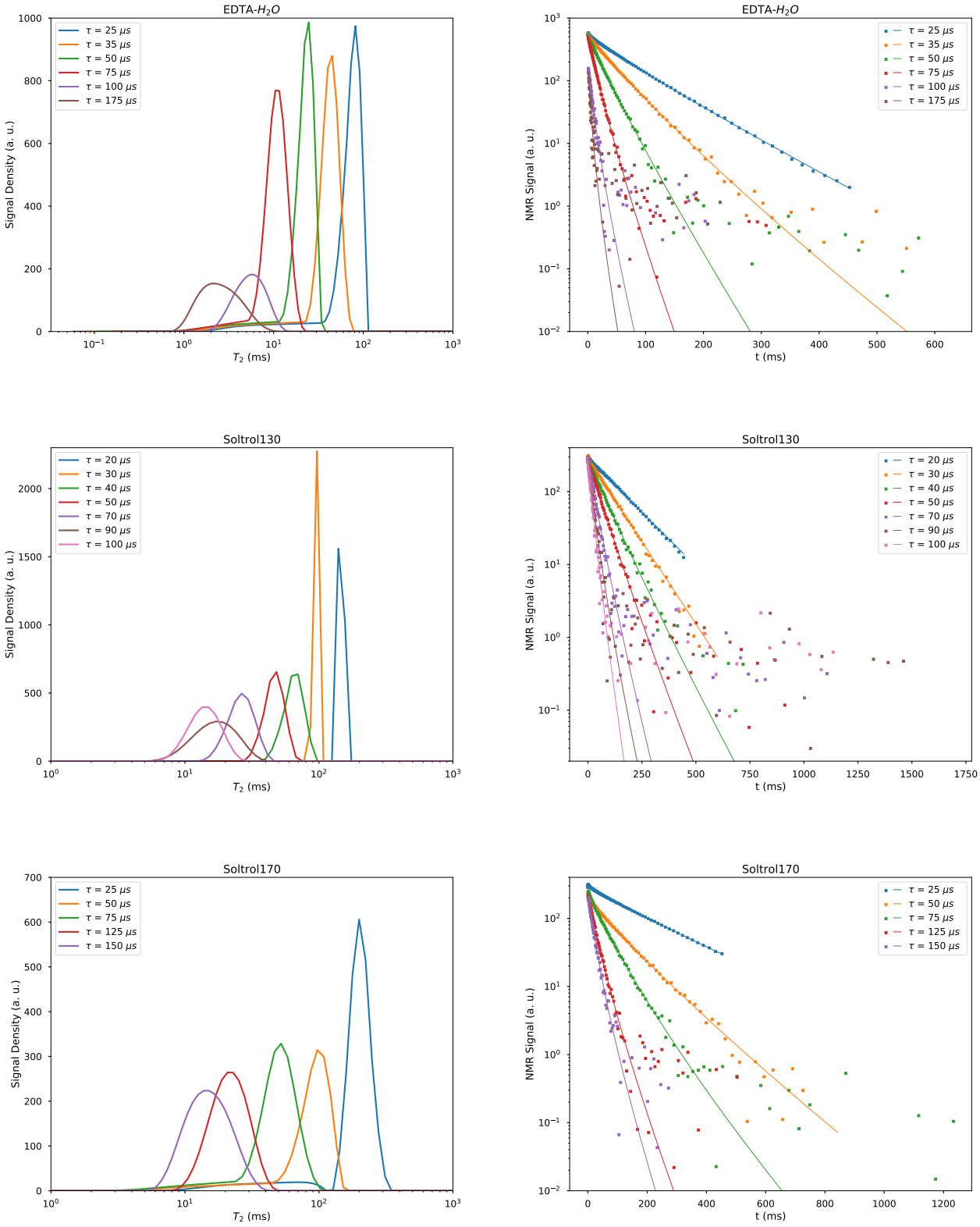

Figure 29. Left side: distribution of T_2^{obs} obtained by UPEN; Right side: NMR Signal data points and mono-exponential fit obtained by UPEN.